



Instrumental investigation of oxygen isotopes in human dental enamel from the Bronze Age battlefield site at Tollense, Germany

T. Douglas Price^{a,*}, Michael J. Spicuzza^b, Ian J. Orland^b, John W. Valley^b

^a Laboratory for Archaeological Chemistry, University of Wisconsin-Madison, United States

^b Department of Geoscience, University of Wisconsin-Madison, United States

ARTICLE INFO

Keywords:

Archaeology
Human proveniencing
Tooth enamel
Oxygen isotopes
Diagenesis
Confocal laser fluorescence microscopy (CLFM)
Secondary ion mass spectrometry (SIMS)

ABSTRACT

Oxygen isotopes were analyzed in human teeth dating to approximately 1250 BC from a Bronze Age battlefield along the Tollense River in northwestern Germany. Tooth enamel was sectioned, prepared, and analyzed using Secondary Ion Mass Spectrometry (SIMS) and Confocal Laser Fluorescence Microscopy (CLFM). The results of the study indicate that diagenesis has locally altered the tooth enamel. Brightly luminescing domains seen by confocal laser fluorescent microscopy are chemically changed in oxygen isotope ratios and elemental [Cl] concentrations. Values of $\delta^{18}\text{O}$ are up to 2.7‰ lower in altered domains. Thus, diagenetic changes are observed in enamel that is 3250 years old and has been waterlogged for most of its depositional history. We recommend that studies of enamel in human teeth routinely evaluate the possibility of diagenesis.

1. Introduction

This study concerns questions about the preservation and alteration of stable isotope ratios and chemical composition in tooth enamel. We first introduce the issues of enamel formation, diagenesis, and oxygen isotopes in apatite. Next, we describe the archaeological site at Tollense, discuss the distinctive nature of the deposits, and the original oxygen isotope investigation of tooth enamel from the site. We then outline new procedures for the analysis of oxygen isotopes in human tooth enamel. A brief description of the instruments that were used in the investigation of the samples follows. Next we describe the samples used in this study and the preparation procedures that were employed. The results of the instrumental investigation are presented in narrative, photographic and graphic form to document changes in the samples that we believe are related to diagenesis. Our study concludes with a discussion of the significance of the results and some suggestions for future research.

2. Tooth enamel formation

Human tooth enamel formation and growth follows known or predictable patterns with appositional layers deposited in onion-like fashion (Fincham et al., 1999; Kang et al., 2004). Enamel development and mineralization is carried out by cells called ameloblasts that form a

single cell layer that covers the developing enamel and is responsible for enamel composition. These ameloblast cells move together to lay down a protein-rich matrix that provides a blueprint for crystal growth (Lacruz et al., 2017). This process begins at the tip of the tooth cusp and continues to the cervix at the enamel-root junction. Thus, the earliest enamel to form is at the cusp and the latest at the root. This layer of ameloblasts obtains nutrients and building materials from the blood stream in the dentine and builds lines of hydroxyapatite ($\text{Ca}_{10}(\text{PO}_4)_6(\text{OH})_2$) on the enamel surface. Enamel is largely composed of hydroxyapatite (with minor substitution of F^- , Cl^- and CO_3^{2-}) and contains no collagen. Once formed it is devoid of any cells, so it cannot remodel (Lacruz et al., 2017). Formation times for various teeth in human dentition are well documented in the literature of oral biology (e.g., Nanci, 2008; Hillson, 2005; Manjunatha and Soni, 2014; Schour and Massler, 1941).

The finished enamel has a characteristic prismatic appearance composed of rods (or prisms), each formed by a single ameloblast, running parallel to the length of the tooth (Nanci, 2008; Raue et al., 2012). The process of formation leaves regular, incremental microscopic bands in the tissue, perpendicular to the elongated axis of the prisms, that are probably due to metabolic variation in the secretion of ameloblasts (Boyde, 1976; Boyde et al., 1988; Dean, 2000; Risnes, 1986). These variations produce short- and long-period incremental (growth) lines in the enamel (Mahoney, 2008). Long-period growth

* Corresponding author.

E-mail addresses: tdprice@wisc.edu (T.D. Price), spicuzza@geology.wisc.edu (M.J. Spicuzza), orland@geology.wisc.edu (I.J. Orland), valley@geology.wisc.edu (J.W. Valley).

<https://doi.org/10.1016/j.jas.2019.03.003>

Received 29 May 2018; Received in revised form 3 March 2019; Accepted 12 March 2019

0305-4403/© 2019 Elsevier Ltd. All rights reserved.

lines are known as the striae of Retzius and form every 6–12 days during human enamel formation (Schwartz et al., 2001; Reid and Ferrell, 2006). Smith (2006, 2008) has provided new evidence for the periodicity of these incremental structures. Antoine et al. (2009) presented convincing evidence that the short-term growth bands (cross-striations) reflect a circadian pattern of daily formation. Counts of these bands provide a chronology for reconstructing development in archaeological human dentition. Many studies rely on the periodicity of this cross-banding. Le Cabec et al. (2015), for example, utilized this information to determine crown formation time and age at death in juvenile fossil Australopithecine hominins from South Africa dating to more than 1 mya.

One of the challenging aspects of enamel formation in humans involves sampling strategies for obtaining information on life history, especially diet and mobility. Although age of formation and development of the enamel can be determined, there are a number of problems remaining regarding the location of enamel of specific age that can be used to estimate a particular point in the early life of an individual. For example, determination of seasonal variation in diet or migration would be very useful information, but to date attempts to isolate enamel from such specific episodes of time have not yet been successful in humans. One problem lies in the technology necessary to locate and sample such minute areas of enamel; another major problem involves the appositional growth process whereby thin layers of enamel are deposited one on top of another over time with intergrowth between the layers. Nevertheless, seasonality has been resolved in $\delta^{18}\text{O}$ of tooth enamel from large mammals (Kohn et al., 1998) and time-averaging was minimized by *in situ* SIMS analysis of aprismatic enamel < 20 μm from the enamel-dentine junction in a laboratory-reared rat (Blumenthal et al., 2014).

3. Tooth enamel diagenesis

There are also potential problems due to diagenesis (e.g., Budd et al., 2000; Nelson et al., 1986; Pollard, 2011; Schoeninger et al., 2003; Sharp et al., 2000; Shin and Hedges, 2012), although little agreement on their scope. Renewed interest in the subject has followed the increasing number of isotopic studies of human remains (e.g., Balter and Zazzo, 2014; Kendall, 2018). Most discussions have focused on carbon and strontium isotopes with relatively little attention to oxygen. There has been a general assumption that the hardness and impermeable nature of enamel retards or prevents contamination. Studies have produced various pro and con arguments. Enamel is clearly denser and more crystalline than bone or dentine and more resistant to post-mortem alteration (e.g., Hoppe et al., 2003; Lee-Thorp and van der Merwe, 1991; Lee-Thorp and Sponheimer, 2003; Sponheimer and Lee-Thorp 1999), but enamel does not always escape diagenetic change. Most examples of diagenetic alteration occur in enamel from ancient sites, greater than 1 m.y. in age, in contexts where skeletal remains were in the process of fossilization. Whether more recent human teeth undergo such significant change is unknown; diagenesis is rarely reported in such cases.

A variety of chemical, instrumental, and imaging techniques have been applied to the question of diagenesis in human remains without firm answers. There are two general groups of such studies, one focused on modern teeth with an orientation toward dental issues and a second concerned with past dentition and aimed at archaeological questions. Most of these studies employ bone or enamel powder in the analysis rather than whole tissue. Rink et al. (1995) used Electron Spin Resonance to examine carbonate in tooth enamel and found limited evidence of diagenesis (2 of 11 samples). Zazzo (2014) using radiocarbon to compare materials concluded that the $\delta^{13}\text{C}$ record measured in bone apatite is probably as reliable as that in enamel for at least the past 40,000 years.

More recently, sampling has been done in three dimensions to try and resolve questions regarding diagenesis in tooth and bone. These

studies focus on micro-sampling or direct analyses using micro-ablation to study the distribution of elemental or isotopic values (e.g., Aubert et al., 2012; Brady et al., 2008; Cerling and Sharp, 1996; Duval et al., 2011; Olivares et al., 2008; Reiche et al., 1999, 2002; Thomas et al., 2011). Al-Jawad et al. (2007) used micro CT scanning to look at enamel formation and lattice parameters. Similar techniques have been applied to archaeological teeth (Montgomery et al., 2012). Simmons et al. (2011, 2013) have used synchrotron X-ray diffraction to map the process of biomineralization and X-ray microtomography to study mineral content distribution in the formation of human enamel. Aubert et al. (2012), Blumenthal et al. (2014), and Beasley et al. (2017) used SIMS (Secondary-Ion Mass Spectrometer) to make high spatial-resolution *in situ* micro-analyses of oxygen isotopes in teeth and other materials. Lebon et al. (2014) utilized Attenuated Total Reflection - Fourier-Transform Infrared Spectroscopy (ATR-FTIR) mapping of bone to document better preservation in the center of cortical bone and taphonomical uptake of carbonate in the most external part of the bone. Ségalen et al. (2008) used cathodoluminescence to map trace element distribution in fossil remains. These studies demonstrated that different mineralized tissues (enamel vs. bone, dentine and cement) and their structure influence the uptake of trace elements during diagenesis (Gaschen et al., 2008; Hinz and Kohn, 2010). In general, the range of variation observed in tooth enamel was much smaller than in other materials and argued for less diagenesis in the enamel.

According to Balter and Zazzo (2014), the molecular and structural properties of the mineral fraction in fossil bone have been widely investigated by means of scanning and transmission electron microscopy (SEM/TEM), X-ray diffraction (XRD) and small angle X-ray scattering (SAXS) as well as infrared (FTIR) and Raman spectroscopy (Person et al., 1995; Reiche et al., 2002; Turner-Walker and Syversen, 2002; Hiller et al., 2003; Pucéat et al., 2004). These studies document the impact of recrystallization processes in creating an increase in apatite crystallinity and a decrease in carbonate content.

4. Oxygen isotopes in apatite

Oxygen isotope ratios vary geographically and seasonally in surface water and rainfall. The oxygen isotope ratio in the human skeleton reflects that of body water, and ultimately of drinking water (Kohn, 1996; Kohn et al., 1998; Luz et al., 1984; Luz and Kolodny, 1985), which in turn predominantly reflects local rainfall. Isotopes in rainfall are greatly affected by enrichment or depletion of the heavy isotope (^{18}O) relative to the lighter ^{16}O in water due to evaporation and precipitation (e.g., Dansgaard, 1964). Major geographic factors affecting rainfall isotope ratios then are latitude, elevation, amount of precipitation, and distance from the source (e.g., an ocean). Rainwater (H_2O) contains five stable isotopes, including ^{16}O and ^{18}O . Molecules of H_2^{18}O have a greater mass than H_2^{16}O and require more energy to evaporate and to stay in the atmosphere. As moisture moves over land, the first precipitation contains more of the heavy isotope and as clouds move inland, to cooler regions, and to higher elevations, the rain becomes more depleted in the heavier isotope (lower in $\delta^{18}\text{O}$, Bowen and Wilkinson, 2002). Thus, oxygen isotope ratios in teeth vary geographically and have potential to provide information on past human movement by comparing place of tooth formation (childhood) and place of death (Bowen and Revenaugh, 2003).

Oxygen isotopes in ancient human skeletal remains have been analyzed from both tooth enamel and bone (France and Owsley, 2015). Oxygen is incorporated into dental enamel during the early life of an individual and should remain unchanged in that enamel through adulthood. Oxygen has three stable isotopes, ^{16}O (99.762% in nature), ^{17}O (0.038%), and ^{18}O (0.2%), all of which are stable and non-radioactive. Oxygen isotopes are conventionally reported as the per mil difference (‰) in the ratio of ^{18}O to ^{16}O between a sample and a standard. This value is designated as $\delta^{18}\text{O}$. This value can be measured either from isolated carbonate (CO_3)⁻² or phosphate (PO_4)⁻³ components in

apatite in tooth and bone, or in both components together. The standards used are commonly VSMOW (Vienna Standard Mean Ocean Water) for phosphate oxygen, water (and sometimes carbonate oxygen) and VPDB (Vienna PeeDee Belemnite) for carbonate oxygen (O'Neil, 1986). Samples are typically ground or drilled to form powder for analysis at mm-scale; less sample is needed for analysis of the carbonate component, preparation is less demanding, and results between laboratories are more comparable (e.g., Bryant and Froelich, 1995, Sponheimer and Lee-Thorp 1999). However, there is a significant oxygen isotope fractionation between the carbonate and phosphate sites in apatite (Aufort et al., 2017). The phosphate component is less labile and may preserve original compositions more faithfully, although this issue is also subject to debate. There is also substantial discussion of appropriate preparation methods for both carbonate and phosphate $\delta^{18}\text{O}$ analyses (Vennemann et al., 2002; Grimes and Pellegrini, 2013; Koch et al., 1997; Pellegrini and Snoeck, 2016).

The $\delta^{18}\text{O}$ values for carbonate and phosphate oxygen in enamel vs. $\delta^{18}\text{O}$ of water can be estimated assuming equilibration at body temperature and converting for different standards (VSMOW vs. VPDB). Chenery et al. (2012) compared $\delta^{18}\text{O}$ values of phosphate and carbonate for 51 archeological samples and derived a relationship between the $\delta^{18}\text{O}_{\text{VSMOW}}$ value of drinking water (DW) and $\delta^{18}\text{O}_{\text{VSMOW}}$ in enamel carbonate (EC) as $\delta^{18}\text{O}(\text{EC}) = (\delta^{18}\text{O}(\text{DW}) + 48.63)/1.59$. Measurements reported relative to the VPDB can be converted to the VSMOW scale: $\delta^{18}\text{O}_{\text{VPDB}} = (0.97001 \times \delta^{18}\text{O}_{\text{VSMOW}}) - 29.99\text{‰}$ (Kim et al., 2015). Thus, as an example, a drinking water $\delta^{18}\text{O}_{\text{VSMOW}}$ value of -6.0‰ yields an estimated enamel carbonate $\delta^{18}\text{O}(\text{EC})_{\text{VSMOW}}$ value of approximately 26.8‰. The exact formula for correlating water to tooth enamel, and methods of oxygen isotope ratio measurement are still debated (Iacumin et al., 1996; Pollard et al., 2011; Pryor et al., 2014).

There are other difficulties in the application of oxygen isotope ratios to human proveniencing (e.g., Daux et al., 2008; Knudson and Price, 2007; White et al., 2004). Many of these issues are raised in a recent essay by Lightfoot and O'Connell (2016). In our own studies, unexplained variation on the order of $\pm 2\text{‰}$ in $\delta^{18}\text{O}$ values among individuals from the same location has been observed (c.f., Evans et al., 2012; Huertas et al., 1995; Lightfoot and O'Connell, 2016). Oxygen isotope ratios of meteoric water vary with latitude, but variation is most pronounced in the polar regions. Many places in the temperate and tropical zones have similar $\delta^{18}\text{O}$ values, ranging broadly from approximately -2.0‰ to -8.0‰ VSMOW, so that finding meaningful differences in these regions can be difficult (Bowen and Revenaugh, 2003; Lightfoot and O'Connell, 2016). Rainfall $\delta^{18}\text{O}$ values vary from season to season, year to year, and over time in the same area (e.g., Rozanski et al., 1993) and such variation can be recorded within a single tooth (Kohn et al., 1998). This variability is undoubtedly a major contributor to the broad range of $\delta^{18}\text{O}(\text{EC})$ values seen at a given site (Lightfoot and O'Connell, 2016).

Moreover, the $\delta^{18}\text{O}$ of human tissue may differ from that of rain falling in the same landscape. Several different factors appear to affect the final values measured in the human skeleton. There are reservoir effects. Water in lakes, ponds, and storage vessels can have higher $\delta^{18}\text{O}$ values due to evaporation of the lighter isotope. Through-flowing rivers can have $\delta^{18}\text{O}$ that differs from local rainfall values. Sources of drinking water may vary locally and result in greater variation in the human population. Cultural practices, such as long-term water storage, cooking, diet, and beverage preparation can influence the $\delta^{18}\text{O}$ of human skeletal tissues (e.g., Brettell et al., 2012; Evans et al., 2012; Knudson and Stojanowski, 2008). There is fractionation of oxygen isotopes during lactation that results in an observable change in $\delta^{18}\text{O}$ (EC) (e.g., Britton et al., 2015; Wright and Schwarcz, 1999).

5. The present study: $\delta^{18}\text{O}$ in tooth enamel

Oxygen isotopes can help resolve questions regarding human mobility. However, in spite of decades of research on the nature and extent

of diagenesis in tooth enamel, it is still not clear how pervasive alteration of the original biogenic signal may be. Because of unexplained variation in oxygen isotope ratios, the application of this method for provenience studies must be done with caution and remains experimental in many regions. In the following pages we report on our CLFM/SIMS investigation of enamel composition and formation. CLFM/SIMS is a powerful new approach that combines detailed confocal laser fluorescence microscopy (CLFM) with *in situ* analysis of oxygen isotope ratios by secondary ion mass spectrometry (SIMS; Orland et al., 2009). Samples came from the human remains at the Bronze Age battlefield site of Tollense in eastern Germany. There was substantial variation in oxygen isotope ratios reported from this site (Price et al., 2017). In this section we describe the archaeological context of the samples, the results of bulk sample oxygen isotope analysis, the methods used in the present study including the instrumentation, the preparation of samples, and the results we obtained. The study concludes with some interpretations of the results and their meaning for the use of oxygen isotope ratios in human proveniencing.

5.1. The archaeological context

The Tollense River in northeast Germany (Fig. 1) flows gently through a low, rolling landscape typical of the North European Plain, flattened by the passage of glaciers during the Ice Age and covered with glacial moraine and sand at the close of the Pleistocene. Since the 1980s there have been occasional finds of bronze artifacts and human remains both in and along several kilometers of the river. The distribution of finds in the river valley is complex: there are *in situ* finds in the river itself as well as on land, but prehistoric materials were also discovered in secondary position in sediments that had been dredged from the river decades ago.

Archaeological excavations and surveys along the valley bottom and

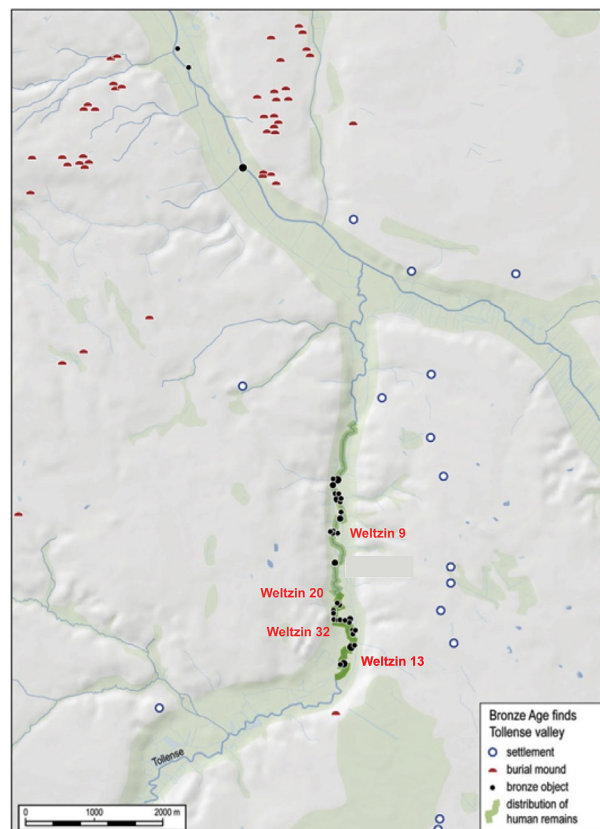


Fig. 1. The Tollense Valley in northeast Germany and the distribution of Bronze Age finds.



Fig. 2. Find layer with human skeletal remains during excavation at site of Weltzin 20.

in the river itself since 2009 have uncovered significant quantities of materials from the Bronze Age, dated to approximately 1250 BC (Lidke et al., 2018). More than 400 m² of the find layer, containing substantial human remains, were excavated on the valley bottom at the main site of Weltzin 20 (Fig. 2), while skeletal material from other localities came mostly from underwater surveys. Human remains are abundant and include a skull cap with an arrowhead deeply buried in the occipital bone. The remains of horses associated with the battle have been found. Metal finds have come largely from detector surveys and include tools and weapons such as knives, arrowheads, spearheads, adzes, daggers and sword fragments. Wooden clubs and other organic materials have also been preserved in the wet deposits of the site.

The find layer is best documented at the locality designated as Weltzin 20, situated on an alluvial fan where materials are preserved approximately 1–1.5 m below present ground level. Here, the bodies of those that perished were apparently looted after the battle and left in a swampy environment. During decomposition processes in shallow water, some skeletal elements were moved slightly by the current. Some of the skeletal remains are more completely preserved in the Bronze Age river bed, more than 2.5 m below present ground level. Partly articulated skeletal elements and the presence of small bones indicate that fluvial transport of bones was limited.

The remains at Tollense would appear to be the result of a large battle. The vast majority of the dead are young adult males and there are a substantial number of perimortem wounds and trauma that must be a result of conflict. The presence of many weapons also would seem to confirm the battlefield nature of the finds. It is important to reiterate the waterlogged conditions in which these materials were found. The human remains were found in the stream and at depth along the banks. These bodies would likely have decomposed on or near the surface of the ground and then gradually have been incorporated in the deposits

of the stream. It seems likely that these remains have been in close association with groundwater and/or the waters of the river until they were removed during the archaeological investigations. This continual exposure to water over several millennia may help to explain the results of this study. The pH values of the Tollense River show strong influences from regional ground water, which is rich in carbonates, and the Lake Tollense where the river originates. The values vary between pH 6.5–8.0 depending on the season (decreasing CO₂ saturation during summer), the influence of organic acids in surrounding mires as well as the sedimentary configuration of the river channel (peat, till, sand) (Sebastian Lorenz, personal communication, 2018).

5.2. Original oxygen isotope analysis at Tollense

We originally sampled 52 teeth from the Tollense valley sites (Weltzin 9, 13, 20, and 32) that are associated with the Bronze Age battle. The analyzed human teeth were largely premolars, but molars or canine teeth were used when premolars were not available. Approximately 20 mg of enamel was collected from each tooth after lightly scouring the outer surface of the enamel in order to remove potential contaminants. Strontium, carbon, oxygen, lead isotope ratios, and Pb concentrations were measured on many of these samples and are described elsewhere (Price, 2014; 2017). Strontium and $\delta^{18}\text{O}$ (EC)_{VSMOW} data from those studies are provided for comparison in Table 1 in this study. Values of $\delta^{18}\text{O}$ (EC) are also reported relative to the VPDB scale in Table 1 to ease comparison with studies that use this standard.

Oxygen was measured by acid dissolution and gas-source mass spectrometry in the carbonate-apatite component of tooth enamel (enamel carbonate, EC) from a bulk sample of apatite from the enamel of 52 individuals (Price et al., 2017). Teeth for the simultaneous analysis of $\delta^{13}\text{C}$ and $\delta^{18}\text{O}$ were chemically cleaned using a standard procedure (Balasse et al., 2002). Enamel samples were placed in approximately 2 mL of 2–3% (v/v) solution of bleach for 8 h and rinsed three times with deionized water, centrifuging the tubes between each aliquot. Then, 0.1 ml/mg of 0.1 M acetic acid was added to each tube for exactly 4 h at room temperature, and the samples were rinsed again with three aliquots of deionized water before being freeze-dried for analysis. Analysis of stable light isotopes was performed in the Environmental Isotope Laboratory (Department of Geosciences, University of Arizona) using a Kiel device attached to a Finnigan MAT252 gas-source mass spectrometer. Samples are converted to CO₂ with concentrated phosphoric acid at 70 °C. External precision, as calculated from repeated measurements of standard reference materials (NBS-18 & NBS-19) is $\pm 0.08\text{‰}$ for $\delta^{13}\text{C}$ and $\pm 0.1\text{‰}$ for $\delta^{18}\text{O}$.

The oxygen isotope ratios measured by gas-source mass spectrometry for the 23 samples in this study range from 24.7 to 27.9‰ VSMOW and the average $\delta^{18}\text{O}$ (EC) value is $+25.8 \pm 1.5\text{‰}$ (2 s.d., n = 23, Price et al., 2017). These $\delta^{18}\text{O}$ values are for enamel carbonate with a VSMOW standard. Subsequent calculation of the rainwater $\delta^{18}\text{O}$ via the empirical relationship described earlier (Chenery et al., 2012) produces a mean value for the samples from the Tollense Valley of approximately -7.6‰ VSMOW, which matches inferred values from the isoscape map of modern rainfall $\delta^{18}\text{O}$ in northwest Germany in Fig. 3 (Tutken et al., 2004). However, the range of $\delta^{18}\text{O}$ (EC) values from 24.7 to 27.9‰ represents significant differences in the childhood homes of these warriors. The map indicates that values of $\delta^{18}\text{O}$ (rain water) in the Tollense Valley area should be on the order of -7.5 to -8.1 , or around 25.5 to 25.9‰ for $\delta^{18}\text{O}$ (EC)_{VSMOW}.

6. Methods of present study

In preparation for CLFM and SIMS, small pieces of tooth enamel from 23 samples previously studied by Price et al. (2017) were cast in epoxy along with UWA-1 apatite standard (metamorphic fluorapatite, Blumenthal et al., 2014) within 5 mm of the center of 25 mm diameter

Table 1

Values measured for $\delta^{13}\text{C}$ and $\delta^{18}\text{O}$ for the human enamel samples from Tollense using both conventional and SIMS methods. Carbon and oxygen isotope ratios from the original study (Price et al., 2017) were measured using conventional methods, described earlier. Sr, C, and O-isotope data for Tollense tooth enamel.

Sample #	$^{87}\text{Sr}/^{86}\text{Sr}$	$\delta^{13}\text{C}(\text{carb})$ Ave.		$\delta^{18}\text{O}(\text{carb})$ Ave.		SIMS $\delta^{18}\text{O}$ Ave.		n	SIMS $\delta^{18}\text{O}$ Ave.	
		Phosphoric		Phosphoric		dark CLFM zones			bright CLFM zones	
		Price 2017		Price 2017		This Study			This Study	
		% PDB	% SMOW	% PDB	% SMOW	% PDB	% SMOW		% PDB	
F6794	0.707422	-7.74	25.40	-5.34	15.7	-14.1	2	15.5	-14.2	2
F6796	0.710968	-8.19	26.57	-4.21	16.7	-13.1	2	16.1	-13.7	2
F6797	0.708580	-8.85	25.31	-5.43	16.1	-13.7	3	15.6	-14.1	1
F6798	0.715014	-5.77	26.06	-4.70	17.7	-12.1	7	16.7	-13.1	4
F6802	0.709184	-9.02	26.08	-4.69	17.0	-12.8	2	14.3	-15.4	2
F6805	0.711513	-10.81	26.08	-4.68	16.9	-12.9	2	16.0	-13.7	2
F6806	0.709464	-11.61	25.95	-4.81	16.1	-13.6	1	15.3	-14.4	2
F6808	0.713669	-5.80	26.90	-3.88	17.8	-12.1	3			
F6809	0.709786	-10.58	25.21	-5.52	16.0	-13.7	3	15.2	-14.5	2
F6810	0.711619	-10.69	25.47	-5.28	16.4	-13.3	3	15.9	-13.8	3
F6811	0.712930	-13.48	27.90	-2.92	19.7	-10.2	5	18.0	-11.8	4
F6812	0.708356	-10.25	25.53	-5.21	16.6	-13.2	2			0
F6813	0.710909	-9.60	24.66	-6.06	14.9	-14.8	3	14.5	-15.2	2
F8412	0.712860	-6.23	25.85	-4.91	16.7	-13.1	2	16.7	-13.0	2
F8414	0.712859	-7.78	26.10	-4.66	17.1	-12.7	2			
F9374	0.710681	-9.86	25.02	-5.71	16.3	-13.4	2	16.3	-13.4	2
F9376	0.710759	-9.87	25.50	-5.24	16.4	-13.4	2	16.1	-13.6	2
F9377	0.709724	-9.14	25.22	-5.52	16.5	-13.3	2	16.6	-13.2	1
F9378	0.710162	-12.38	26.57	-4.21	17.5	-12.3	2	17.4	-12.4	2
F9380	0.709325	-7.85	25.10	-5.64	16.0	-13.7	2	14.9	-14.9	2
F9382	0.708125	-7.59	25.99	-4.77	16.6	-13.2	2	16.4	-13.4	2
F9385	0.709516	-9.89	25.26	-5.48	16.2	-13.6	3	14.9	-14.9	2
F9386	0.708254	-9.27	24.85	-5.87	15.7	-14.0	2	14.8	-14.9	3

Sample #'s are the same as in Price et al. (2017).

CLFM = Confocal laser fluorescence microscopy.

Phosphoric = Conventional analysis of carbonate component of bulk apatite in enamel by acid digestion.

From Price et al., 2017).

SIMS $\delta^{18}\text{O}$ spot analysis (~10 μm spot) reflects oxygen in phosphate, OH and carbonate component of apatite.

n = number of spot analyses.

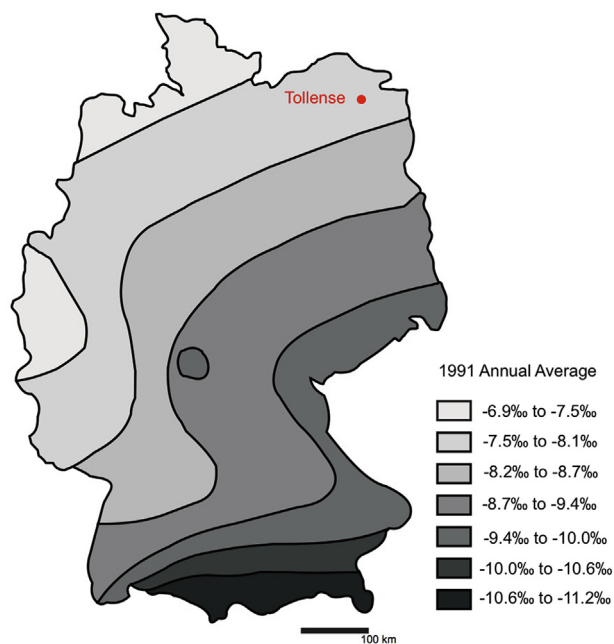


Fig. 3. An isoscape for 1991 annual average rainfall $\delta^{18}\text{O}_{\text{VSMOW}}$ values in Germany (Tutken et al., 2004). The map also shows the location of the Tollense sites in northeast Germany.

mounts, ground, and polished to a smooth planar surface with polishing relief < 2 μm . Typically, the exposed and polished surfaces of each sample measure 1–2 mm in length. These samples were imaged by confocal laser scanning fluorescence microscopy prior to analysis by SIMS, and by SEM after analysis. For SIMS analysis, the sample surface was thinly coated with gold, which was subsequently removed, and a thin carbon coat applied before SEM imaging.

6.1. Confocal laser fluorescence microscopy

Confocal laser scanning fluorescence microscopy (CLFM) uses pinhole apertures and optical filters to select and constrain laser-excited fluorescence (Carlsson et al., 1985). The pinholes are configured to select the sample-emitted fluorescence so that only in-focus emission reaches the detector, rejecting the majority of the out-of-focus light. The depth-discriminating property of confocal microscopy can be used to carry out optical slicing of specimens in order to generate a three-dimensional raster covering a volume of the specimen (e.g. Schopf and Kudryavtsev, 2009). The brightness and contrast of the fluorescence images can be enhanced digitally. The instrument used in this study was a Bio-Rad MRC-1024 scanning confocal microscope at the University of Wisconsin-Madison Keck Bioimaging Laboratory using settings detailed by Orland et al. (2009). A laser with 488 nm wavelength excited fluorescence in the samples, and the emitted light was filtered to permit wavelengths between 505 and 539 nm.

6.2. Secondary ion mass spectrometry (SIMS)

Secondary Ion Mass Spectrometry is used to analyze the composition of solids by sputtering shallow pits into the surface of the specimen

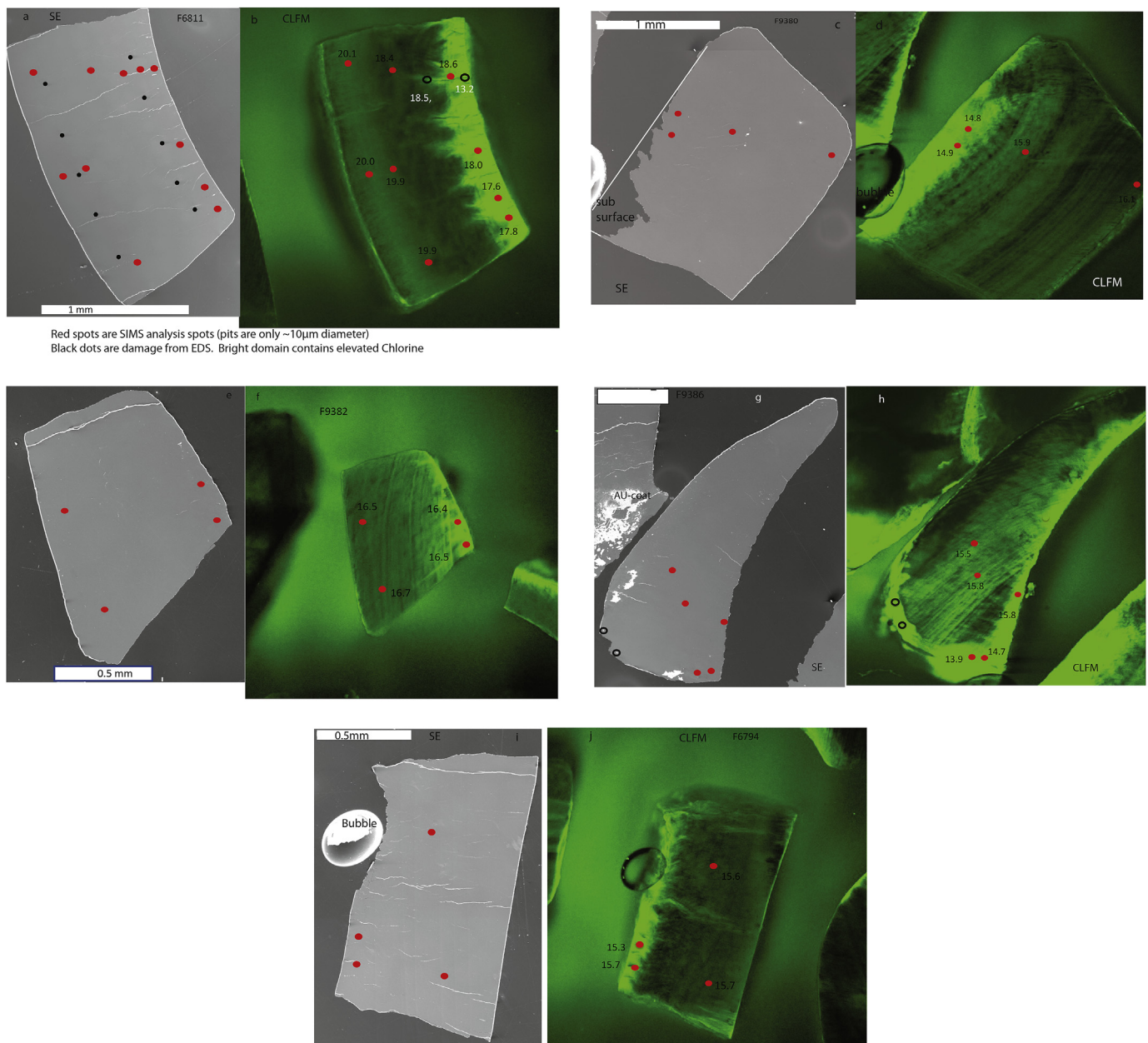


Fig. 4. Matching images by SEM-SE (scanning electron microscopy-secondary electrons) and CLFM (confocal laser fluorescent microscopy) of five samples of tooth enamel from Tollense showing oxygen isotope values (VSMOW) measured *in situ* from 10 μm spots (red dots) by SIMS (secondary ion mass spectrometry). Open black circles are irregular SIMS pits (see text). Black dots are spots from SEM-EDS. The bright domains by CLFM contain elevated [Cl]. Note that some areas covered by epoxy fluoresce by CLFM and are outlined in white in SE images. Chips and cracks in SE are sometimes white due to charging. (a,b) Sample F6811. (c,d) Sample F9380. (e,f) Sample 9382. (g,h) Sample F9386. (i,j) Sample F6794. (For interpretation of the references to colour in this figure legend, the reader is referred to the Web version of this article.)

with a focused primary ion beam and collecting and analyzing ejected secondary ions. The mass/charge ratios of these secondary ions are measured with a mass spectrometer to determine the elemental, isotopic, or molecular composition. SIMS is a very sensitive analysis technique, with elemental detection limits ranging from parts per million to parts per billion.

Oxygen isotope analyses were performed with a CAMECA (Paris, France) IMS-1280 large radius, multi-collector ion microprobe at the WiscSIMS Laboratory, Department of Geoscience, University of Wisconsin–Madison using a $^{133}\text{Cs}^+$ primary ion beam with an accelerating voltage of 10 kV, impact energy of 20 keV and a beam current of ~ 1.8 nA, focused to a 10- μm beam-spot size (Kita et al., 2009, 2011, Valley and Kita, 2009). Charge neutralization was assisted by a low-

energy electron gun and a coating of gold on the sample surface. Sample spots were placed within tooth enamel, guided by CLFM images (Fig. 4). Analytical conditions were comparable to those previously reported at WiscSIMS (Kozdon et al., 2009; Orland et al., 2009) with the addition of simultaneous OH measurement; secondary ions were detected simultaneously by 3F cups ($^{16}\text{O}^-$, $^{16}\text{O}^1\text{H}^-$, $^{18}\text{O}^-$). The count rates for $^{16}\text{O}^-$ were $\sim 2.3 \times 10^9$ cps. The total analytical time per spot was 3 min including pre-sputtering, automatic centering of the secondary ion image in the field aperture and analysis (4 s \times 20 cycles = 80 s). Grains of UWA-1 were mounted with random orientations in the center of the sample and were measured as a running standard in at least four spots before and four spots after every 12–16 sample analyses. The resulting average $\delta^{18}\text{O}$ value of UWA-1 measurements

bracketing the samples was used for instrumental bias and drift correction. Reproducibility of the bracketing UWA-1 standard measurements is assigned as analytical precision of unknown samples; the mean spot-to-spot reproducibility is 0.28‰ 2 SD (varying from 0.14‰ to 0.41‰). All measured SIMS data are reported in App. 1 data linked to this paper and summarized in Table 1.

Due to the large variation in matrix effects among different materials, accurate SIMS analysis requires the use of comparison standards. The authors do not know of a homogeneous sample of tooth enamel that is calibrated and suitable for use as a SIMS standard for $\delta^{18}\text{O}$. They have investigated many potential samples and are still searching. In this study, UWA-1 is used both as a running standard and for calibration. It is assigned a value of $\delta^{18}\text{O} = +12.7 \pm 0.4\text{‰}$ VPDB (2SD, $n = 2$) that was determined for laser fluorination of two untreated chips (T. Vennemann, pers. comm., 2013). This value represents all oxygen in the standard. Because UWA-1 is a metamorphic fluorapatite, the hydrous and carbonate components are thought to be negligible, which is verified by six TC-EA analyses of Ag_3PO_4 prepared from UWA-1 that yielded $\delta^{18}\text{O} = 12.8 \pm 0.4\text{‰}$ VSMOW (2SD, Vennemann, pers. comm., 2013). However, tooth enamel contains a small component of carbonate- and OH-apatite and thus its composition differs from UWA-1. There is no better way to make this correction at present and the SIMS $\delta^{18}\text{O}$ values may show a small systematic error as a result. It is important to recognize that if an error exists in calibration, it will be the same for all of the SIMS data reported in this study. Measurements of the magnitude of differences between different samples or across zoning are robust.

6.3. Scanning electron microscopy

After SIMS analysis, the gold coating was removed, and the sample mount was coated with carbon and imaged for secondary electrons (SE), backscattered electrons (BSE), and cathodoluminescence (CL) by scanning electron microscopy (SEM) using a Hitachi S-3400N variable-pressure SEM equipped with a Gatan CL system (PanaCL) in high vacuum mode. Enamel in this study had very weak or no CL response. Sample F6811 was also analyzed for differences in elemental composition by semi-quantitative energy dispersive X-ray spectrometry (EDS, Oxford x-act). Ten spots (five in CLFM-bright and five in CLFM-dark areas) were counted for a total of 30 s/each with an accelerating voltage of 15 kV.

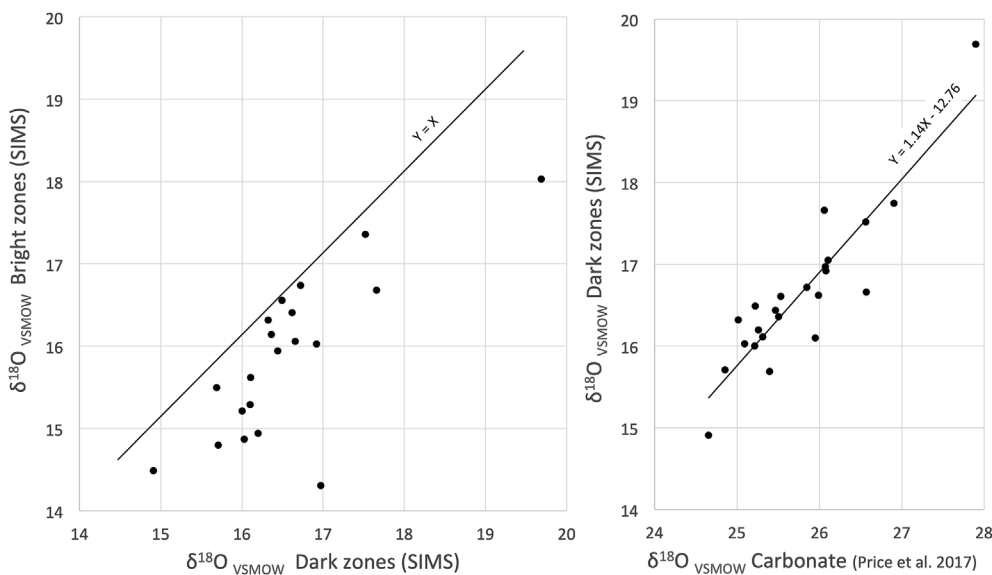


Fig. 5. Oxygen isotope ratios measured in 23 samples of tooth enamel by acid extraction of powder and *in situ* by SIMS (secondary ion mass spectrometry). (a) *In situ* analyses of altered domains fluorescing brightly vs. those with dark or growth-zoned fluorescence. (b) *In situ* analyses of dark domains vs. data measured by acid-extraction of the carbonate apatite component of enamel.

7. Results

For the present study we selected a total of 23 teeth for CLFM imaging and SIMS analysis in order to image internal zoning and obtain detailed spot measurements of oxygen isotope ratios within the enamel. Values for $\delta^{18}\text{O}$ obtained with the SIMS are plotted on CLFM images for selected samples in Fig. 4. Photos of all samples are shown with labeled SIMS pits in App. 2 of Supplementary Information. We will present the results in three parts: a description of some of the zonation observed by CLFM, graphical and statistical comparison of the darker and lighter areas in the photos, and comparison of conventional bulk-analysis vs. *in situ* SIMS for $\delta^{18}\text{O}$ values.

The tooth enamel samples examined in this study all show variable patterns of luminescence by CLFM from dark to bright green due to subtle differences in chemistry (Fig. 4, App. 2). EDS analyses of CLFM bright and dark areas in F6811 (Fig. 4a) indicate a small but detectable elevated level of ~ 0.4 wt % chlorine in bright (altered) enamel. However, the most likely cause of bright luminescence is the presence of humic and other organic acids that can be added to water-logged samples by interaction with soil water (Senesi et al., 1991; Orland et al., 2009). The bright domains of this study are concentrated near the edges of enamel exposed to groundwater. The boundaries between bright and dark domains are sometimes sharp, but often gradational. Some samples are also rimmed by thin bright lines on both natural surfaces and surfaces broken during sample preparation. We interpret these thin edge-effects to result from surface contamination during preparation and reflections around the sides of sample chips, and not necessarily to result from intrinsic chemical differences of the enamel itself. This interpretation of thin edge effects is supported by artifacts in the SEM-SE images that show enhanced emission of secondary electrons on edges and cracks causing them to be highlighted by white lines in the SE images. The percentage of brightly luminescing enamel in CLFM varies from approximately 10 to 30%, but some samples have diffuse bright zones throughout the areas imaged. Many samples reveal distinct growth banding in the darker domains that becomes less distinct or disappears in bright domains. In some samples the bright domains clearly cut across this banding and locally the bright domains are seen to follow micro-cracks in enamel.

A total of 116 *in situ* SIMS analyses were made with an average of four spot-analyses per sample (Table 1, App. 1). Post analysis imaging revealed irregularities for 13 analysis pits (identified in App. 1) and 103 analyses are deemed reliable. For comparison, the previously published values of $\delta^{18}\text{O}$, $\delta^{13}\text{C}$ and $^{87}\text{Sr}/^{86}\text{Sr}$ are also reported in Table 1. It is

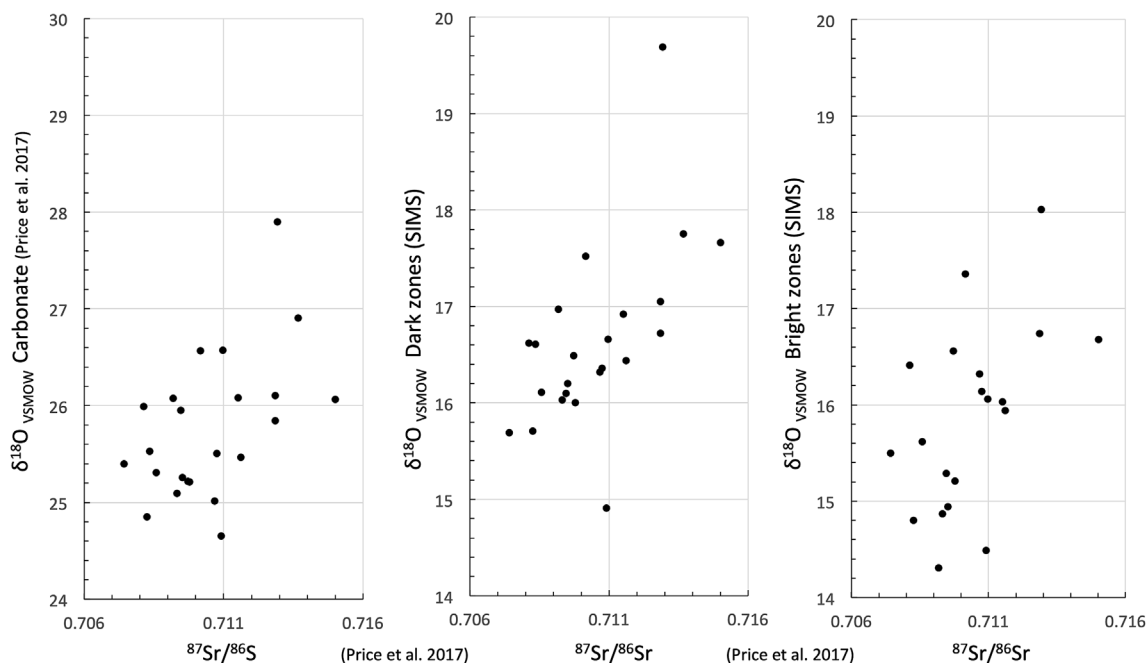


Fig. 6. Values of $\delta^{18}\text{O}$ measured in bulk by acid dissolution and *in situ* by SIMS, plotted against $^{87}\text{Sr}/^{86}\text{Sr}$ ratios for the same samples: (a) conventional measurement using phosphoric acid and gas-source mass spectrometry, (b) SIMS measurement of dark-CLFM, unaltered areas in enamel, (c) SIMS measurement of bright-CLFM, altered areas in human tooth enamel.

important to keep the scale of the photos in mind. The samples analyzed by SIMS were sputtered from pits measuring $\sim 10\ \mu\text{m}$ in diameter by $1\ \mu\text{m}$ deep; the sputtered enamel weighed $\sim 1\ \text{ng}$. In contrast, the published acid-extraction $\delta^{18}\text{O}$ values came from samples more than 10^7 times larger; powdered volumes of tooth enamel were greater than a few mm^3 and weighed 10–100 mg. The values of $\delta^{18}\text{O}$ measured by both techniques are shown in Figs. 5 and 6. The *in situ* SIMS analysis spots targeted both bright- and dark-CLFM domains in each tooth. The $\delta^{18}\text{O}$ values of bright-luminescing domains average $+16.6\text{‰}$ VSMOW and are consistently lower than values for the dark domains that average $+17.4\text{‰}$ (Fig. 5a). On average this difference is 0.8‰ , but the difference is significantly greater, up to 2.7‰ , for some domains.

The $\delta^{18}\text{O}$ values for the dark-CLFM domains by SIMS average 9.2‰ lower than the acid-extraction analyses because the *in situ* analyses include all sources of oxygen from each pit, which includes the phosphate, carbonate, and hydrous components of enamel, while the acid analyses only sample oxygen bonded as CO_3^{2-} in carbonate-apatite, which typically amounts to only a few wt.% of the total oxygen. It is important to remember that the SIMS $\delta^{18}\text{O}$ data are not expected to match the $\delta^{18}\text{O}$ of the acid-extracted CO_3 , which is different than bulk O (measured by SIMS) due to a different bonding environment of PO_4^{3-} vs. CO_3^{2-} and possibly due to different rates of alteration.

8. Discussion

The primary goal of this study is to image tooth enamel samples from Tollense at high magnification and to use *in situ* oxygen isotope analysis by SIMS to determine if the enamel is homogeneous in oxygen isotope ratio and, if not, the cause(s) of variability. Next, we discuss five representative samples (Fig. 4). Each sample is shown with matching images by SEM-SE and by CLFM. The locations of SIMS pits are illustrated with solid red ovals. The few pits that produced irregular analyses are shown with open black ovals.

Sample F6811. Fig. 4b shows a dramatic contrast between the bright and dark areas in enamel fragments. There is no comparable difference in the SE image (4a), except that there are more small cracks in the bright-CLFM domain (white lines) in 4a than in 4b (dark lines). Semi-

quantitative SEM-EDS analysis of elemental composition (black dots, Fig. 4a) consistently shows that [Cl] is below detection in the dark domains and $\sim 0.4\ \text{wt}\%$ Cl in the bright domains. A number of SIMS measurements were made on this piece, both in the bright area and in the dark, presumably unaltered, zone. Four SIMS measurements of $\delta^{18}\text{O}$ in the bright zone average 18.0‰ VSMOW, while the five measurements in the dark zone average 19.7‰ . Two analyses are on a visible crack rimmed by bright luminescence (black ovals in Fig. 4b); one gave an unusually low $\delta^{18}\text{O}$ value of 13.2‰ . It is not certain if this value represents extreme alteration or if the analysis is biased by the irregular location. These two low values are not included in subsequent discussion.

Sample F9380. Fig. 4c and d. The brightly luminescing domain cuts across growth bands. A portion of the left side of the sample in Fig. 4c is covered by a thin layer of epoxy that is darker by SE; this dark feature is not seen in the matching CLFM image (Fig. 4d) because the epoxy is transparent to visible light. Small white spots in the SE image are caused by charging at chips in the surface. Two SIMS measurements of $\delta^{18}\text{O}$ in the bright zone average 14.9‰ VSMOW, while the two measurements in the dark zone average 16.0‰ .

Sample F9382. Fig. 4e and f. Two SIMS measurements of $\delta^{18}\text{O}$ in the cross-cutting bright zone average 16.4‰ VSMOW, while the two measurements in the dark zone average 16.6‰ .

Sample F9386. Fig. 4g and h have three values in the bright area that surrounds the growth-zoned dark domain that was analyzed twice. Irregularly shaped white areas in the SE image are residual gold coat. The pits from two other analyses in the bright domain are irregular in appearance and these data are considered unreliable (black ovals in Fig. 4h). The three values in the bright area are variable and average $\delta^{18}\text{O} = 14.8\text{‰}$. The two values in the dark zone are the same within uncertainty and average 15.7‰ .

Sample F6794. Fig. 4i and j shows two measurements in the bright area and two in the dark zone. The bright areas that are seen around the outer-edges of the enamel in CLFM are thicker than the thin white lines seen in SE that result from edge-effects. The boundaries between light and dark in CLFM are diffuse and extend along cracks into the interior of the sample. Values for $\delta^{18}\text{O}$ are similar in the dark zone

(average = 15.7‰) vs. the bright zone (average = 15.5‰). The small sphere on the left of this photo is an air bubble in the epoxy.

The outer portions of enamel in all of these examples and others in Appendix 2 are brighter by CLFM. The bright domains correlate to lower $\delta^{18}\text{O}$ by SIMS and increased [Cl] in the one sample that was analyzed. They contain more fine cracks and appear to cut into dark domains along cracks. The cross-cutting relations revealed by CLFM clearly show that the bright domains formed after the growth banding in tooth enamel. We interpret these results to demonstrate that the bright-CLFM domains were altered post-mortem while the samples were exposed to the organic-acid-rich groundwaters or stream water at Tollense. The evidence of this alteration and if it affects the isotopic or chemical composition of enamel was not known at the start of the study. We emphasize that alteration affects the phosphate components of the enamel and not just carbonate. Samples of tooth enamel from the last 100,000 years have typically been assumed to be pristine. Similar altered textures were observed in significantly older (4 mya) teeth from Allia Bay, Kenya by SEM-CL (Schoeninger et al., 2003) and by CLFM (Beasley, 2016). To our knowledge, this is the first report of such alteration in younger samples.

It is tempting to calculate the conditions of alteration based on the new SIMS data. If enamel reached isotopic equilibrium with groundwater, then the temperatures of exchange and the $\delta^{18}\text{O}$ of the water would be constrained. However, the irregular variability of SIMS $\delta^{18}\text{O}$ values measured in bright domains shows that isotope equilibrium was not attained during the post-mortem alteration. Furthermore, it's not presently known if the alteration is homogeneous within the 10- μm domains analyzed by SIMS, concentrated along grain boundaries of apatite crystallites or possibly involves precipitation of new nm-size phases (Gordon et al., 2015). Thus, while it's likely that water had a value near average rainwater and that temperatures were in the range of 20 °C, any quantitative calculation of the process of alteration is speculative.

Plots of measured $\delta^{18}\text{O}$ values are enlightening. Fig. 5a shows the relation of average $\delta^{18}\text{O}$ for the dark domain of each sample vs. for the bright domain for the 20 samples that have data for both domains. Although some samples show little difference, 50% of the samples differ significantly, and bright domains are systematically lower in $\delta^{18}\text{O}$ by up to 2.7‰. Clearly, the alteration of $\delta^{18}\text{O}$ has heterogeneously lowered the $\delta^{18}\text{O}$ of bright domains in tooth enamel. It is likely that the intensity of alteration is affected by the local environment of burial, including depth, soil type, saturation of sediments, mixture of soil water vs. river water, and temperature. The values of $\delta^{18}\text{O}$ for apparently unaltered dark domains correlate well with the values of carbonate-apatite measured by acid extraction of bulk powders (Fig. 5b). However, the slope of this correlation is not one to one. The dark domains show a greater range (4.6‰) than the range of bulk analyses (3.1‰). Presumably the conventional analysis of large powdered samples has averaged the altered and the pristine domains and the *in situ* SIMS analysis reveals a more accurate value for the pre-mortem tooth.

Fig. 6 plots $\delta^{18}\text{O}$ vs. $^{87}\text{Sr}/^{86}\text{Sr}$ in three graphs. Fig. 6a shows $\delta^{18}\text{O}$ (EC) for bulk samples of tooth enamel reacted with phosphoric acid (Price et al., 2017). Fig. 6b and c shows the *in situ* SIMS data for the unaltered dark and the altered bright domains, respectively. The SIMS data for unaltered spots show the largest range and tightest fit to a line. The SIMS data for altered spots show more scatter. Both the conventional acid extraction data and the unaltered SIMS data from tiny spots indicate a correlation between $\delta^{18}\text{O}$ and the strontium isotope ratios which fits with a more northerly origin for some of the participants in the battle at Tollense.

9. Conclusions

It is clear that the tooth enamel in this study was diagenetically altered as chemical changes can be seen in the prepared, polished samples. Domains that luminesce brightly by CLFM are concentrated in

the outer parts of enamel that were exposed to groundwater, are chemically changed and have systematically lower oxygen isotope ratios than the darker interior enamel, which appears unchanged or less altered. Thus, diagenetic alteration can be documented in phosphate portions of enamel that is less than 4000 years old and has been waterlogged for most of its depositional history. Only the *in situ* $\delta^{18}\text{O}$ data for the dark CLFM domains are truly accurate for proveniencing. It is important to note that these diagenetic changes are relatively small in the samples examined from Tollense and may contribute less than half of the overall variability that is witnessed in oxygen isotope proveniencing by bulk analysis. It is also important to remember that preparation of sample powder has the effect of mixing altered and unaltered domains prior to analysis. It is the case that diagenesis would not have affected our conclusions in the original investigation of Tollense. However, other samples from other localities may experience more substantial alteration. It cannot be assumed that the carbonate or the phosphate components of tooth enamel are pristine in buried samples without independent verification.

Acknowledgements

This project began as a collaboration between Valley and Price. Valley, a geochemist, had noticed the variation in oxygen isotopes in enamel reported in the initial publication of the isotopic investigation of the human remains found at the Bronze Age battlefield site at Tollense in northeast Germany (Jantzen et al., 2011, 2014; Price 2014, 2017). Price, an archaeologist, had known Valley for many years at UW-Madison and the two had previously collaborated. Valley is the founder of WiscSIMS (the Wisconsin Secondary Ion Mass Spectrometer Laboratory) that operates an instrument that allows spot measurements of light isotopes at very high resolution. Price was the founder of the Laboratory for Archaeological Chemistry at UW-Madison. Our goal was to measure oxygen isotope ratios in various areas of the enamel to see if there was patterning related to formation, growth, or any other factors. Spicuzza is a colleague of Valley and did much of the preparation and instrumental work involved in this project and observed and recorded the evidence for enamel diagenesis that we report here. Orland is responsible for CLFM analysis and contributed significantly to this manuscript.

WiscSIMS is supported by NSF (EAR-1355590, -1658823) and the UW-Madison. JWV and MJS are supported by NSF (EAR-1524336). We thank the following for their assistance at UW-Madison: Brian Hess (sample preparation); John Fournelle and Bil Schneider (SEM); Noriko Kita, and Kouki Kitajima (SIMS). The original oxygen measurements by acid reaction of bulk enamel (Price et al., 2017) were done by David Dettman at the University of Arizona, Department of Geosciences.

Research at these remarkable find spots in the Tollense Valley has been carried out since 2007, directed by the Landesamt für Kultur und Denkmalpflege, Department of Archäologische Denkmalpflege and the department of Ur-und Frühgeschichte of the University of Greifswald, supported since 2009 by the Ministry of Education, Science and Culture of Mecklenburg-Western Pomerania (Jantzen et al., 2011) and since 2010 by the Deutsche Forschungsgemeinschaft (German Research Foundation). The project is directed by Detlef Janzen and Thomas Terberger. Special thanks also to Terberger and Gundula Lidke for their help with this manuscript.

Appendix A. Supplementary data

Supplementary data to this article can be found online at <https://doi.org/10.1016/j.jas.2019.03.003>.

References

- Al-Jawad, Maisoon, Steuwer, Axel., Kilcoyne, Susan H., Shore, Roger C., Cywinski, Robert, Wood, David J., 2007. 2D mapping of texture and lattice parameters of dental

- enamel. *Biomaterials* 28, 2908–2914.
- Antoine, Daniel, Hillson, Simon, Christopher Dean, M., 2009. The developmental clock of dental enamel: a test for the periodicity of prism cross-striations in modern humans and an evaluation of the most likely sources of error in histological studies of this kind. *J. Anat.* 214, 45–55.
- Aubert, M., Pike, A.W.G., Stringer, C., Bartsiakos, A., Kinsley, L., Eggins, S., Day, M., Grün, R., 2012. Confirmation of a late middle Pleistocene age for the Omo Kibish 1 cranium by direct uranium-series dating. *J. Hum. Evol.* 63, 704–710.
- Aufort, J., Segalen, L., Gervais, C., Paulatto, L., Blanchard, M., Balan, E., 2017. Site-specific equilibrium isotopic fractionation of oxygen, carbon, and calcium in apatite. *Geochem. Cosmochim. Acta* 219, 57–73.
- Balasse, M., Ambrose, S.H., Smith, A.B., Price, T.D., 2002. The seasonal mobility model for prehistoric herders in the south-western Cape of South Africa assessed by isotopic analysis of sheep tooth enamel. *J. Archaeol. Sci.* 29, 917–932.
- Bone and enamel diagenesis: from the crystal to the environment - a tribute to Jean-François Salège. Balter, Vincent, Zazzo, Antoine (Eds.), *Palaeogeogr. Palaeoclimatol. Palaeoecol.* 416, 1–178.
- Beasley, M.M., 2016. *Seasonal Precipitation at a 3.97 Ma Australopithecus anamensis Site, Allia Bay, Kenya*. PhD thesis. Univ. California, San Diego.
- Beasley, M.M., Orland, I.J., Valley, J.W., Schoeninger, M.J., 2017. Understanding Enamel Diagenesis of $\delta^{18}\text{O}$ Using High Resolution SIMS Data and CLFM Imaging. *Bone Diagenesis Conference*, Oxford 2017.
- Blumenthal, Scott A., Cerling, Thure E., Chritz, Kendra L., Bromage, Timothy G., Kozdon, Reinhard, Valley, John W., 2014. Stable isotope time-series in mammalian teeth: in situ $\delta^{18}\text{O}$ from the innermost enamel layer. *Geochem. Cosmochim. Acta* 124, 223–236.
- Bowen, Gabriel J., Revenaugh, Justin, 2003. Interpolating the isotopic composition of modern meteoric precipitation. *Water Resour. Res.* 39, 1299–1311.
- Bowen, Gabriel J., Wilkinson, B., 2002. Spatial distribution of $\delta^{18}\text{O}$ in meteoric precipitation. *Geology* 30 315–8.
- Boyde, A., 1976. Amelogenesis and the structure of enamel. In: Cohen, B., Kramer, I.R.H. (Eds.), *Scientific Foundations of Dentistry*. William Heinemann Medical Books Ltd, London, pp. 335–352.
- Boyde, A., Fortelius, M., Lester, K.S., Martin, L.B., 1988. Basis of the structure and development of mammalian enamel as seen by scanning electron microscopy. *Scanning Microsc.* 2, 1479–1490.
- Brady, A.L., White, C.D., Longstaffe, F.J., Southam, G., 2008. Investigating intra-bone isotopic variations in bioapatite using IR-laser ablation and micromilling: implications for identifying diagenesis? *Palaeogeogr. Palaeoclimatol. Palaeoecol.* 266, 190–199.
- Brettell, R., Montgomery, J., Evans, J., 2012. Brewing and stewing: the effect of culturally mediated behaviour on the oxygen isotope composition of ingested fluids and the implications for human provenance studies. *J. Anal. At. Spectrom.* 27, 778–785.
- Britton, Kate, Fuller, Benjamin T., Tütken, Thomas, Mays, Simon, Michael, P., Richards, 2015. Oxygen isotope analysis of human bone phosphate evidences weaning age in archaeological populations. *Am. J. Phys. Anthropol.* 157, 226–241.
- Bryant, J., Daniel, Froelich, Philip N., 1995. A model of oxygen isotope fractionation in body water of large mammals. *Geochem. Cosmochim. Acta* 59, 4523–4537.
- Budd, P., Montgomery, J., Barreiro, B., Thomas, R.G., 2000. Differential diagenesis of strontium in archaeological human dental tissues. *Appl. Geochem.* 15, 687–694.
- Carlsson, K., Danielsson, P.E., Lenz, R., Liljeborg, A., Majlöf, L., Åslund, N., 1985. Three-dimensional microscopy using a confocal laser scanning microscope. *Optic Lett.* 10 (2), 53–55.
- Cerling, T.E., Sharp, Z.D., 1996. Stable carbon and oxygen isotope analysis of fossil tooth. Stable carbon and oxygen isotope analysis of fossil tooth enamel using laser ablation. *Palaeogeogr. Palaeoclimatol. Palaeoecol.* 126, 173–186.
- Chenery, C.A., Pashley, V., Lamb, A., Sloane, H.J., Evans, J.A., 2012. The oxygen isotope relationship between the phosphate and structural carbonate fractions of human bioapatite. *Rapid Commun. Mass Spectrom.* 26, 309–319.
- Dansgaard, W., 1964. Stable isotopes in precipitation. *Tellus* 16, 466–468.
- Daux, V., Lecuyer, C., Heran, M.-A., Amiot, R., Simon, L., Fourel, F., et al., 2008. Oxygen isotope fractionation between human phosphate and water revisited. *J. Hum. Evol.* 55, 1138–1147.
- Dean, Christopher, 2000. Incremental markings in enamel and dentine: what they can tell us about the way teeth grow. In: Teaford, Mark (Ed.), *Development, Function and Evolution of Teeth*, Mark Ferguson, Moya Smith. Cambridge University Press, New York, pp. 119–130.
- Duval, M., Aubert, M., Hellstrom, J., Grün, R., 2011. High resolution, LA-ICP-MS mapping of U and Th isotopes in an early pleistocene equid tooth from fuente nueva-3 (orce, andalusia, Spain). *Quat. Geochronol.* 6, 458–467.
- Evans, J.A., Chenery, C.A., Montgomery, J., 2012. A summary of strontium and oxygen isotope variation in archaeological human tooth enamel excavated from Britain. *J. Anal. At. Spectrom.* 27, 754–764.
- Fincham, A.G., Moradian-Oldak, J., Simmer, J.P., 1999. The structural biology of the developing dental enamel matrix. *J. Struct. Biol.* 126, 270–299.
- France, C.A.M., Owsley, Douglas W., 2015. Stable carbon and oxygen isotope spacing between bone and tooth collagen and hydroxyapatite in human archaeological remains. *Int. J. Osteoarchaeol.* 25, 299–312.
- Gaschen, A.A.-M., Döbeli, M., Markwitz, A., Barry, B., Ulrich Bochsler, S., Krähenbühl, U., 2008. Restrictions on fluorine depth profiling for exposure age dating in archaeological bones. *J. Archaeol. Sci.* 35, 535–552.
- Gordon, L.M., Cohen, M.J., MacRenaris, K.W., Pasteris, J.D., Seda, T., Derk Joester, D., 2015. Amorphous intergranular phases control the properties of rodent tooth enamel. *Science* 347, 746–750.
- Grimes, V., Pellegrini, M., 2013. A comparison of pretreatment methods for the analysis of phosphate oxygen isotope ratios in bioapatite. *Rapid Commun. Mass Spectrom.* 27, 375–390.
- Hiller, J.C., Thompson, T.H.U., Evison, M.P., Chamberlain, A.T., Wess, T.J., 2003. Bone mineral change during experimental heating: an X-ray scattering investigation. *Biomaterials* 24, 5091–5097.
- Hillson, S., 2005. *Teeth*. Cambridge University Press, Cambridge.
- Hinz, E.A., Kohn, M.J., 2010. The effect of tissue structure and soil chemistry on trace element uptake in fossils. *Geochem. Cosmochim. Acta* 74, 3213–3231.
- Hoppe, K.A., Koch, P.L., Furutani, T.T., 2003. Assessing the preservation of biogenic strontium in fossil bones and tooth enamel. *Int. J. Osteoarchaeol.* 13, 20–28.
- Huertas, A.D., Iacumin, P., Stenni, B., Chillón, B.S., Longinelli, A., 1995. Oxygen-isotope variations of phosphate in mammalian bone and tooth enamel. *Geochem. Cosmochim. Acta* 59, 4299–4305.
- Iacumin, P., Bocherens, H., Mariotti, A., Longinelli, A., 1996. Oxygen isotope analyses of co-existing carbonate and phosphate in biogenic apatite: a way to monitor diagenetic alteration of bone phosphate? *Earth Planet. Sci. Lett.* 142, 1–6.
- Jantzen, Detlef, Brinker, Ute, Orschiedt, Jörg, Jan, Heinemeier, Jürgen, Piek, Hauenstein, Karlheinz, Krüger, Joachim, Lidke, Gundula, Lübke, Harald, Lampe, Reinhard, Lorenz, Sebastian, Schult, Manuela, Terberger, Thomas, 2011. A bronze age battlefield? Weapons and trauma in the Tollense valley, north-eastern Germany. *Antiquity* 85, 417–433.
- Jantzen, Detlef, Lidke, Gundula, Jana, Dräger, Krüger, Joachim, Rassmann, Knut, Lorenz, Sebastian, Terberger, Thomas, 2014. An early Bronze Age causeway in the Tollense Valley, Mecklenburg-Western Pomerania – the starting point of a violent conflict 3300 years ago? *Bericht der Römisch-Germanischen Kommission* 95, 13–49.
- Kang, Daniel, Amarasiwardena, Dulasiri, Alan, H., Goodman, 2004. Application of laser ablation-inductively coupled plasma-mass spectrometry (LA-ICP-MS) to investigate trace metal spatial distributions in human tooth enamel and dentine growth layers and pulp. *Ann. Bioanal. Chem.* 78, 1608–1615.
- Kendall, Christopher, Eriksen, Anne Marie Hoier, Kontopoulos, Ioannis, Collins, Matthew J., Turner-Walker, Gordon, 2018. Diagenesis of archaeological bone and tooth. *Palaeogeogr. Palaeoclimatol. Palaeoecol.* 491, 21–37.
- Kim, S.-T., Coplen, T.B., Horita, J., 2015. Normalization of stable isotope data for carbonate minerals: implementation of IUPAC guidelines. *Geochem. Cosmochim. Acta* 158, 276–289.
- Kita, N.T., Ushikubo, T., Fu, B., Valley, J.W., 2009. High precision SIMS oxygen isotope analysis and the effect of sample topography. *Chem. Geol.* 264, 43–57.
- Kita, N.T., Huberty, J.M., Kozdon, R., Beard, B.L., Valley, J.W., 2011. High precision SIMS oxygen, sulfur and iron stable isotope analyses of geological materials: accuracy, surface topography and crystal orientation. In: *SIMS XVII Proceedings, Surface and Interface Analysis* 43, pp. 427–431.
- Knudson, K.J., Price, T.D., 2007. Utility of multiple chemical techniques in archaeological residence mobility studies: case studies from Tiwanaku- and Chiribaya-affiliated sites in the Andes. *Am. J. Phys. Anthropol.* 132, 25–39.
- Knudson, Kelly J., Stojanowski, M., 2008. New directions in bioarchaeology: recent contributions to the study of human social identities. *J. Archaeol. Res.* 16, 397–432.
- Koch, Paul L., Tuross, Noreen, Fogel, Marilyn L., 1997. The effects of sample treatment and diagenesis on the isotopic integrity of carbonate in biogenic hydroxylapatite. *J. Archaeol. Sci.* 24, 417–429.
- Kohn, M.J., 1996. Predicting animal ^{18}O : accounting for diet and physiological adaptation. *Geochem. Cosmochim. Acta* 60, 4811–4829.
- Kohn, M.J., Schoeninger, M.J., Valley, J.W., 1998. Variability in oxygen isotope compositions of herbivore teeth: reflections of seasonality or developmental physiology? *Chem. Geol.* 152, 97–112.
- Kozdon, R., Ushikubo, T., Kita, N.T., Spicuzza, M., Valley, J.W., 2009. Intratest oxygen isotope variability in the planktonic foraminifer *N. pachyderma*: real vs. apparent vital effects by ion microprobe. *Chem. Geol.* 258, 327–337.
- Lacruz, R.S., Habelitz, S., Wright, J.T., Paine, M.L., 2017. Dental enamel formation and implications for oral health and disease. *Physiol. Rev.* 97, 939–993.
- Le Cabec, A., Tang, N., Taffereau, P., 2015. Accessing developmental information of fossil hominin teeth using new synchrotron microtomography based visualization techniques of dental surfaces and interfaces. *PLoS One* 10 (4), e0123019. <https://doi.org/10.1371/journal.pone.0123019>.
- Lebon, M., Zazzo, A., Reiche, I., 2014. Screening *in situ* bone and teeth preservation by ATR-FTIR mapping. *Palaeogeogr. Palaeoclimatol. Palaeoecol.* 416, 110–119.
- Lee-Thorp, J.A., Sponheimer, M., 2003. Three case studies used to reassess the reliability of fossil bone and enamel isotope signals for paleodietary studies. *J. Anthropol. Archaeol.* 22, 208–216.
- Lee-Thorp, J.A., van der Merwe, N.J., 1991. Aspects of the chemistry of modern and fossil biological apatites. *J. Archaeol. Sci.* 18, 343–354.
- Lidke, Gundula, Jantzen, Detlef, Lorenz, Sebastian, Terberger, Thomas, 2018. The bronze age battlefield in the Tollense valley, northeast Germany – conflict scenario research. In: Fernández-Götz, M., Roymans, N. (Eds.), *Conflict Archaeology. Materialities of Collective Violence from Prehistory to Late Antiquity*. Routledge, Abingdon/New York, pp. 61–68 Themes in Contemporary Archaeology 5.
- Lightfoot, E., O'Connell, T.C., 2016. On the use of biomineral oxygen isotope data to identify human migrants in the archaeological record: intra-sample variation, statistical methods and geographical considerations. *PLoS One* 11 (4), e0153850. <https://doi.org/10.1371/journal.pone.0153850>.
- Luz, B., Kolodny, Y., 1985. Oxygen isotope variations in phosphate of biogenic apatites. IV. Mammal teeth and bones. *Earth Planet. Sci. Lett.* 75, 29–36.
- Luz, B., Kolodny, Y., Horowitz, M., 1984. Fractionation of oxygen isotopes between mammalian bone-phosphate and environmental drinking water. *Geochem. Cosmochim. Acta* 48, 1689–1693.
- Mahoney, Patrick, 2008. Intraspecific variation in M1 enamel development in modern humans: implications for human evolution. *J. Hum. Evol.* 55, 131–147.
- Manjunatha, B.S., Soni, Nishit K., 2014. Estimation of age from development and eruption

- of teeth. *J. Forensic Dent. Sci.* 6 (2), 73–76.
- Montgomery, Janet, Beaumont, Julia, Mackenzie, Kevin, Gledhill, Andrew, Shore, Roger, Brookes, Steven, Salmon, Phil, Lynnerup, Niels, 2012. Timelines in teeth: using micro-CT scans of partially mineralized human teeth to develop a new isotope sampling strategy. *Am. J. Phys. Anthropol.* 147 (Suppl. 54), 216.
- Nanci, A., 2008. *Ten Cate's Oral Histology: Development, Structure, and Function*. Mosby Elsevier, St. Louis.
- Nelson, B.K., Deniro, M.J., Schoeninger, M.J., De Paolo, D.J., Hare, P.E., 1986. Effects of diagenesis on strontium, carbon, nitrogen and oxygen concentration and isotopic composition of bone. *Geochem. Cosmochim. Acta* 50, 1941–1949.
- Olivares, M., Etxebarria, N., Arana, G., Castro, K., Murelaga, X., Berreteaga, A., 2008. Multi-element μ -ED-XRF analysis of vertebrate fossil bones. *X Ray Spectrom.* 37, 293–297.
- Orland, I.J., Bar-Matthews, M., Kita, N.T., Ayalon, A., Matthews, A., Valley, J.W., 2009. Climate deterioration in the eastern Mediterranean from 200 BC to 1100 AD as revealed by ion microprobe analysis of speleothems from Soreq Cave, Israel. *Quat. Res.* 71, 27–35.
- O'Neil, J.R., 1986. Terminology and standards. In: Valley, J.W., Taylor, H.P., O'Neil, J.R. (Eds.), *Stable Isotopes*, vol. 16. Mineralogical Society of America, pp. 561–570. *Reviews in Mineralogy*.
- Pellegrini, M., Snoeck, C., 2016. Comparing bioapatite carbonate pre-treatments for isotopic measurements: Part 2—impact on carbon and oxygen isotope compositions. *Chem. Geol.* 420, 88–96.
- Person, A., Bocherens, H., Saliège, J.-F., Zeitoun, V., Gérard, M., 1995. Early diagenetic evolution of bone phosphate: an X-ray diffractometry analysis. *J. Archaeol. Sci.* 22, 211–221.
- Pollard, A.M., 2011. Isotopes and impact: a cautionary tale. *Antiquity* 85, 631–638.
- Pollard, A.M., Pellegrini, M., Lee-Thorp, J.A., 2011. Technical Note: some observations on the conversion of dental enamel $\delta^{18}\text{O}_\text{p}$ values to $\delta^{18}\text{O}_\text{w}$ to determine human mobility. *Am. J. Phys. Anthropol.* 145, 499–504.
- Price, T., Douglas, 2014. Isotopic analysis of human tooth enamel from the Tollense valley, Germany. A preliminary report. In: Jantzen, D., Orschiedt, J., Piek, J., Terberger, T. (Eds.), *Tod im Tollenseetal — Forschungen zu den Hinterlassenschaften eines bronzezeitlichen Gewaltkonfliktes in Mecklenburg-Vorpommern 1. Die Forschungen bis 2011. Landesamt für Kultur und Denkmalpflege, Schwerin*, pp. 223–232. *Beiträge zur Ur- und Frühgeschichte Mecklenburg-Vorpommerns*.
- Price, T., Douglas, Frei, Robert, Brinker, Ute, Frei, Karin, Jantzen, Detlef, Terberger, Thomas, 2017. Multi-Isotope Analysis of Human Remains from a Bronze Age Battlefield in Northeast Germany. *J. Anthropol. Archaeol. Sci.* <https://doi.org/10.1007/s12520-017-0529-y>.
- Pryor, A.J.E., Stevens, R.E., O'Connell, T.C., Lister, J.R., 2014. Quantification and propagation of errors when converting vertebrate biomineral oxygen isotope data to temperature for palaeoclimate reconstruction. *Palaeogeogr. Palaeoclimatol. Palaeoecol.* 412, 99–107.
- Pucéat, E., Reynard, B., Lécuyer, C., 2004. Can crystallinity be used to determine the degree of chemical alteration of biogenic apatites? *Chem. Geol.*, vol. 205, 83–97.
- Raue, L., Gersdorff, N., Rödiger, M., Klein, H., 2012. New insights in prism orientation within human enamel. *Arch. Oral Biol.* 57, 271–276.
- Reiche, I., Favre-Quattrapani, L., Calligaro, T.J.S., Bocherens, H., Charlet, L., Menu, M., 1999. Trace element composition of archaeological bones and postmortem alteration in the burial environment. *Nucl. Institut. Meth. Phys. Res. B* 150, 656–662.
- Reiche, I., Vignaud, C., Menu, M., 2002. The crystallinity of ancient bone and dentine: new insights by transmission electron microscopy. *Archaeometry* 44, 447–459.
- Reid, D.J., Ferrell, R., 2006. The relationship between number of striae of Retzius and their periodicity in imbricational enamel formation. *J. Hum. Evol.* 50, 195–202.
- Rink, W.J., Schwartz, H.P., Smith, F.H., Radovic, J., 1995. ESR dating of tooth enamel from Neanderthal site of Krapina, Croatia. *Nature* 378, 24–26.
- Risnes, S., 1986. Enamel apposition rate and the prism periodicity in human teeth. *Scand. J. Dent. Res.* 94, 394–404.
- Rozanski, K., Araguás-Araguás, L., Gonfiantini, R., 1993. Isotopic patterns in modern global precipitation. In: Swart, P.K., Lohmann, K.C., McKenzie, J.A., Savin, S. (Eds.), *Climate Change in Continental Isotopic Records*. American Geophysical Union, Washington DC, pp. 1–36.
- Schoeninger, M.J., Hallin, K., Valley, J.W., Fournelle, J., 2003. Isotopic alteration of mammalian tooth enamel. *Int. J. Osteoarcheol.* 13, 11–19.
- Schopf, J.W., Kudryavtsev, A.B., 2009. Confocal laser scanning microscopy and Raman imagery of ancient microscopic fossils. *Precambrian Res.* 173, 39–49.
- Schour, I., Massler, M., 1941. The development of the human dentition. *JADA (J. Am. Dent. Assoc.)* 28, 1153–1160.
- Schwartz, G.T., Reid, D., Dean, C., 2001. Developmental aspects of sexual dimorphism in hominoid canines. *Int. J. Primatol.* 22, 837–860.
- Ségalen, Loïc, De Rafélis, Marc, Lee-Thorp, Julia A., Maurer, Anne-France, Renard, Maurice, 2008. Cathodoluminescence tools provide clues to depositional history in Miocene and Pliocene mammalian teeth. *Palaeogeogr. Palaeoclimatol. Palaeoecol.* 266, 246–253.
- Senesi, Nicola, Miano, Teodoro, Provenzano, Maria R., Brunetti, Gennaro, 1991. Characterization, differentiation, and classification of humic substances by fluorescence spectroscopy. *Soil Sci.* 152, 259–271.
- Sharp, Z.D., Atudorei, V., Furrer, H., 2000. The effect of diagenesis on oxygen isotope ratios of biogenic phosphates. *Am. J. Sci.* 300, 222–237.
- Shin, J.Y., Hedges, R.E.M., 2012. Diagenesis in bone and enamel apatite carbonate: the potential of density separation to assess the original composition. *J. Archaeol. Sci.* 39, 1123–1130.
- Simmons, L.M., Al-Jawad, M., Kilcoyne, S.H., Wood, D.J., 2011. Distribution of enamel crystallite orientation through an entire tooth crown studied using synchrotron X-ray diffraction. *Eur. J. Oral Sci.* 119 (Suppl. 1), 19–24.
- Simmons, Lisa M., Montgomery, Janet, Beaumont, Julia, Davis, Graham R., Al-Jawad, Maisoon, 2013. Mapping the spatial and temporal progression of human dental enamel biomineralization using synchrotron X-ray diffraction. *Arch. Oral Biol.* 58, 1726–1734.
- Smith, Tanya M., 2006. Experimental determination of the periodicity of incremental features in enamel. *J. Anat.* 208, 99–113.
- Smith, Tanya M., 2008. Incremental dental development: methods and applications in hominoid evolutionary studies. *J. Hum. Evol.* 54, 205–224.
- Sponheimer, M., Lee-Thorp, J., 1999. Oxygen isotopes in enamel carbonate and their ecological significance. *J. Archaeol. Sci.* 26, 723–728.
- Thomas, D.B., McGovern, C.M., Fordyce, R.E., Frew, R.D., Gordon, K.C., 2011. Raman spectroscopy of fossil bioapatite—a proxy for diagenetic alteration of the oxygen isotope composition. *Palaeogeogr. Palaeoclimatol. Palaeoecol.* 310, 62–70.
- Turner-Walker, G., Syversen, U., 2002. Quantifying histological changes in archaeological bones using BSE-SEM image analysis. *Archaeometry* 43, 461–468.
- Tu'tken, T., Pfretzschner, H.-U., Vennemann, T.W., Sun, G., Wang, Y.D., 2004. Paleobiology and skeletochronology of Jurassic dinosaurs: implications from the histology and oxygen isotope compositions of bones. *Palaeogeogr. Palaeoclimatol. Palaeoecol.* 206 (3–4), 217–238.
- Valley, J.W., Kita, N.T., 2009. In situ oxygen isotope geochemistry by ion microprobe. In: Fayek, M. (Ed.), *GAC/MAC Short Course: Secondary Ion Mass Spectrometry in the Earth and Planetary Sciences* 41. Mineralogical Association of Canada, Toronto, pp. 19–63.
- Vennemann, T.W., Fricke, H.C., Blake, R.E., O'Neil, J.R., Colman, A., 2002. Oxygen isotope analysis of phosphates: a comparison of techniques for analysis of Ag_3PO_4 . *Chem. Geol.* 185, 321–336.
- White, C.D., Storey, R., Longstaffe, F.J., Spence, M.W., 2004. Immigration, assimilation, and status in the ancient city of Teotihuacan: stable isotopic evidence from Tlajinga. *Lat. Am. Antiq.* 33, 176–198.
- Wright, L.E., Schwarcz, H.P., 1999. Correspondence between stable carbon, oxygen and nitrogen isotopes in human tooth enamel and dentine: infant diets and weaning at Kaminaljuyú. *J. Archaeol. Sci.* 26, 1159–1170.
- Zazzo, Antoine, 2014. Bone and enamel carbonate diagenesis: a radiocarbon prospective. *Palaeogeogr. Palaeoclimatol. Palaeoecol.* 16, 168–178.